

Differential Diffusion: Giving Each Pixel Its Strength

ERAN LEVIN, Tel Aviv University, Israel

OHAD FRIED, Reichman University, Israel

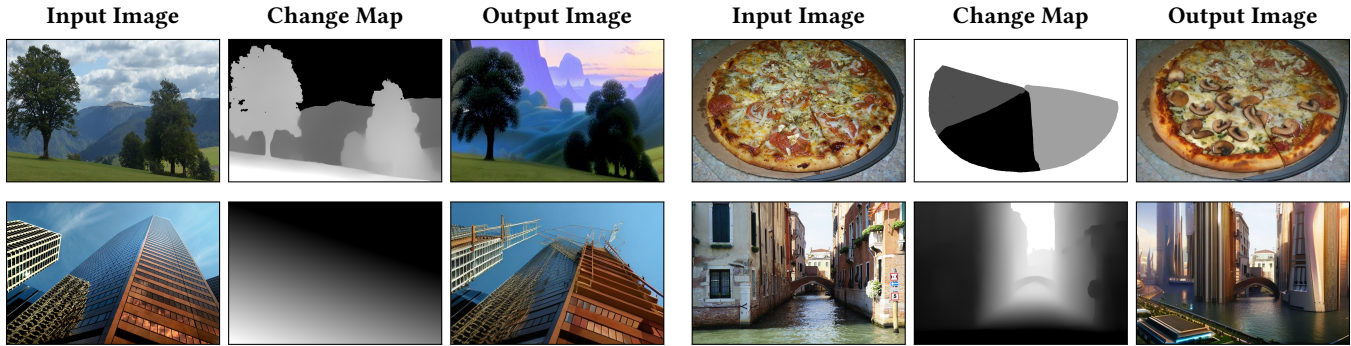


Fig. 1. Applications of our method: Localized Style Transfer, Heterogeneous Editing, Convey Progression, Augmenting Reality. The prompts are (left to right, top to bottom): “a detailed matte painting...”, “a bunch of mushrooms on a pizza”, “scaffolding”, “a futuristic city with tall buildings...”. See the appendix for the full prompts.

Text-based image editing has advanced significantly in recent years. With the rise of diffusion models, image editing via textual instructions has become ubiquitous. Unfortunately, current models lack the ability to customize the *quantity* of the change per pixel or *per image fragment*, resorting to changing the entire image in an equal amount, or editing a specific region using a binary mask. In this paper, we suggest a new framework which enables the user to customize the quantity of change for each image fragment, thereby enhancing the flexibility and verbosity of modern diffusion models. Our framework does not require model training or fine-tuning, but instead performs everything at inference time, making it easily applicable to an existing model. We show both qualitatively and quantitatively that our method allows better controllability and can produce results which are unattainable by existing models. Our code is available at: <https://github.com/exx8/differential-diffusion>.

CCS Concepts: • **Computing methodologies** → **Image-based rendering**; *Mixed / augmented reality*.

Additional Key Words and Phrases: diffusion models, differential diffusion, image editing

1 INTRODUCTION

If you want to edit an image, many options are available. Besides traditional approaches such as manual editing via Photoshop, modern AI tools are at your service. For example, you can edit your image via text instructions [Brooks et al. 2023]. The most successful image generators that were developed in recent years use a diffusion process [Rombach et al. 2022a; Saharia et al. 2022], and in many of these models you can configure the amount of change made to the picture. But what if you want to edit a fragment (a specific region of the picture)? In works such as Blended Diffusion [Avrahami et al. 2022b], you can select which fragments of the picture to edit binarily. However, it is, at most, a binary choice. When you edit

a picture, you can only specify one amount of change (which is usually termed “strength”). Fragments of the image are changed by the same strength, or not changed at all. This is limiting. Sometimes, an editor wishes to change different regions of the image in different amounts. For example, if you add mushrooms to a pizza, you might want to add for different slices a different amount of mushrooms. In another example, given a photo of a person, instead of limiting yourself to zombifying the entire person, you might want to zombify different body parts in different amounts, indicating a progressive decaying process.

Furthermore, sometimes the editor wishes to have a continuous transition between adjacent fragments. This is sometimes visually more favorable and photo-realistic.

We present a novel technique for prompt-based image editing, which enables a user to determine the strength of editing each pixel in the image, thus controlling which parts of the image will remain as-is, and which will be changed *and by how much*. Unlike previous methods, we allow the user to choose the quantity of change in a non-binary fashion, thus enabling greater flexibility and finer-grained editing of the image. We make key observations (Section 3.2) that allow us to create an efficient inference process (Section 3.4). Our technique does not require training or fine-tuning, and it only adds minimal overhead to the inference process Table 2. We demonstrate several applications of our method, and evaluate it against several baselines (Section 4). Our main contributions are:

- We define new methods to manipulate the inference process of diffusion models. See: Sections 3.4 and 3.4.2.
- We utilize them for creating a new inference process which is capable of editing a picture by different quantities according to a map – Algorithm 1.
- We suggested a new metric for comparing different techniques according to their adherents for such maps.

Authors’ addresses: Eran Levin, eran.levin@cs.tau.ac.il, Tel Aviv University, Kiryat HaUniversita, Ramat Aviv P.O. Box 39040, Tel Aviv, Israel, 6997801; Ohad Fried, Reichman University, PO Box 167, 8 Ha’universita Street, herzliya, Israel, ofried@runi.ac.il.

2 RELATED WORK

Our method performs text-based image to image translation. We first review methods that generate complete images from text (Section 2.1), and then describe image-to-image translation methods using either text (Section 2.2.1) or masks (Section 2.2.2) as input.

2.1 Text-based Image Synthesis

Research on text-based image generation has become ubiquitous. Early models such as DRAW [Gregor et al. 2015] and alignDRAW [Mansimov et al. 2016], while impressive, tended to produce blurry outputs. Many GAN-based [Goodfellow et al. 2014] models were proposed [Arjovsky et al. 2017; Liu et al. 2021; Reed et al. 2016; Sauer et al. 2023; Xu et al. 2017; Zhang et al. 2022, 2017], which produce higher quality output, but they often lack coherence—they sometimes missed hierarchical structures which led complex object to be blurry [Reed et al. 2016].

Recently, diffusion models [Ho et al. 2020; Sohl-Dickstein et al. 2015] have emerged as a leading solution for image generation [Dhariwal and Nichol 2021; Nichol and Dhariwal 2021], and for text-to-image synthesis [Patashnik et al. 2021; Zhang et al. 2023]. Stable Diffusion [Rombach et al. 2022a] has gained attention from the research community, industry, and the public, in part because the researchers chose to freely release the model’s checkpoints¹.

Our method is an image-to-image translation technique, and it does not attempt to synthesize images from scratch. It builds on the above synthesis methods, specifically diffusion models.

2.2 Inpainting

Palette [Saharia et al. 2022] introduced a diffusion-based model, which solves four tasks: colorization, cropping, JPEG restoration, and inpainting — the ability to discard and re-synthesize parts of an image, in a photo-realistic way. While inpainting does allow editing of a specific region, in contrast to our solution it always discards the selected content completely. Also, Palette does not allow the user to guide the completion content by any mean. Stable Diffusion-2 [Stability AI Ltd 2023] offers guided inpainting, taking as input a binary edit mask, a guiding text, and a strength parameter. However, it does not allow specifying different strengths in the same transformation. Also, it requires fine-tuning, in contrary to our solution. Therefore, these solutions, and other inpainting approaches [Kim et al. 2022a; Lugmayr et al. 2022; Quan et al. 2022; Suvorov et al. 2022; Yu et al. 2023], offer minimal control on the strength along the picture of the changed fragments, in contrary to our method.

2.2.1 Text-based Editing. Several approaches take an image as input, and use text to guide an editing process. DiffusionCLIP [Kim et al. 2022b] uses domain-specific diffusion models, DDIM inversion, and fine-tuning for image editing. “More Control for Free!” [Liu et al. 2022] has suggested a framework for semantic image generation which allow guiding it simultaneously with a text and an image. Prompt-to-prompt [Hertz et al. 2022] has suggested text-based editing images by DDIM inversion and modifying cross attention layers. Textual Inversion [Gal et al. 2022], DreamBooth [Ruiz et al. 2022]

¹We hope that other researchers (and companies) will choose to do the same. Our code and models are available at <https://github.com/exx8/differential-diffusion>.

allows personalizing the generation process, to a specific subject. Allowing the user to retain some concepts of an image in a new image. Text2LIVE [Bar-Tal et al. 2022] enables to add visual effects as well as editing a texture of a picture by a prompt. Imagic [Kawar et al. 2023] enables to edit an image semantically via a prompt.

InstructPix2Pix [Brooks et al. 2023] enables the user to edit pictures with human friendly instructions, which in turn are translated to prompts.

All the methods produce impressive results, but most don’t allow the user to specify a change-quantity, and all don’t allow the user to select directly on the picture which fragments of the picture to change. Giving free rein to the model to decide how much each fragment of the picture should change.

2.2.2 Mask-based Editing. SDEdit [Meng et al. 2022] offers stroke-base editing by using a GAN [Goodfellow et al. 2014]. Blended Diffusion [Avrahami et al. 2022a,b] can edit specific image fragments using a diffusion model [Ho et al. 2020; Rombach et al. 2022b; Sohl-Dickstein et al. 2015]. Unfortunately, They all lack two key features we suggest: (1) Control the strength of change. In the described methods, users can discard a fragment completely or not. On our framework, user can choose to keep some qualities of the original figure by configuring the corresponding strength. (2) Different fragment can get different strengths, meaning different object in the picture can change in a different quantity.

Our work can be viewed as a generalization of stroke-based editing. When given a binary mask (instead of a fractional mask), our method acts similarly to the methods above.

3 METHOD

Given an image, a mono-channel change map representing the strength of editing in each pixel, and a text prompt to guide the edit, we aim to edit the image. We want the generated result to satisfy the strength constraints, be photo-realistic, and adhere to the prompt.

3.1 Overview

Diffusion models are deep machine learning models that have been inspired by thermodynamics [Sohl-Dickstein et al. 2015]. In computer vision context, they are usually trained gradually to denoise images, that have been corrupted by a random Gaussian noise. Usually the image-to-image translation process (“**the inference process**”) begins with an image with added Gaussian noise, then in a repetitive process the noise is gradually removed. This inference process creates a series of images, where each is the result of the denoising process of the previous one (“**the inference chain**”).

The **prompt** is a text that describes the content of the generated segments. **Strength** is a parameter that guides the amount of change in an image. See: Figure 5. For more details, see Saharia et al. [2022]. Usually there is a single strength parameter for the entire image. In this work we allow different strengths for each fragment of the image, via the **change map**, or simply “the map” — a tensor with the height and width of the original image, with values between 0 and 1, representing the strength to apply to each pixel. In contrast to previous works [Avrahami et al. 2022a,b], we denote a complete change as “black” (0) and not “white” (1).

In Latent Diffusion Models [Rombach et al. 2022b], the **latent encoder** is a neural network that compresses an image into a smaller latent space, in which we apply the diffusion process. At the end of the process, a **latent decoder** decompress the latent output into an image.

In this work, we present *Differential Diffusion* — an enhancement of image-to-image diffusion models that adds the ability to control the amount of change applied to each image fragment via a change map (Algorithm 1). The method only changes the inference process.

Algorithm 1 Differential Image to Image Diffusion

Input x (image to edit), k (number of steps), μ (change map between 0 and 1), p (prompt)

Output \hat{x}

```

1: procedure INFERENCE( $x, k, \mu, p$ )
2:    $z_{init} = \text{ldm\_encode}(x)$ 
3:    $\mu_s = \text{down\_sample}(\mu)$ 
4:    $z'_k = \text{add\_noise}(z_{init}, k)$ 
5:    $z_k = \text{denoise}(z'_k, p, k)$ 
6:   for  $t = k - 1$  to  $0$  do
7:      $z'_t = \text{add\_noise}(z_{init}, t)$ 
8:      $mask = \mu_s \otimes \frac{t}{k}$ 
9:      $z_t^{mix} = z_{t+1} \odot mask + z'_t \odot (1 - mask)$ 
10:     $z_t = \text{denoise}(z_t^{mix}, p, t)$ 
11:  end for
12:   $\hat{x} = \text{ldm\_decode}(z_0)$ 
13:  return  $\hat{x}$ 
14: end procedure

```

Whereas \otimes , \odot are element-wise larger-than and element-wise multiplication, respectively. \otimes returns a tensor of 1s and 0s.

3.2 Observations

For designing the algorithm we made three key-observations:

- (1) Given two series of indices of time-steps (100, 95, ...), of two inference process, A and B, created by the same parameters, up to the strength parameter; without loss of generality, let the inference process of A be with a higher strength than B. Then $B \subseteq A$. Furthermore $\exists i \geq 0 (\forall j \geq 0 (B[j] = A[i + j]))$. Meaning, B is a truncated series of A.
- (2) One can insert a fragment of a picture, which is encoded to the latent space, into an intermediate step t of the chain, without breaking the inference process, by inserting the fragment with noise that corresponds to t . In Figure 2 we show the effects of such insertion on intermediate steps via our Algorithm 1. We will call this an **injection**.
- (3) The latent encoder that we use (Stable Diffusion [Rombach et al. 2022a]) generally encodes pixels to the same relative positions, meaning for non-miniscule shapes in the picture, one can estimate which position they will be in the latent-tensor, just by calculating their relative positions. We call this property **locality**.

Our algorithm is composed of the following techniques:

3.3 Change Map Down-Sampling

The map is down-sampled to match the size of the latent-space encoding, by height and width (the same map is applied to all the channels), as the diffusion process is preformed in the latent-space, and not in the pixel space. Due to locality, the down-sampled map matches the position of the latent pixel in the latent tensor.

3.4 Fragment Injection

We define a new operation called injection — the process of replacing fragments in the latent space. As we replace fragments in the noised latent space, we must inject segments that are encoded and noised according to the current time-step.

3.4.1 Gradual Injection. We inject the fragments in a time-step and noise that match their user-specified change map. Fragments with the smallest strength value are added last, and with the least amount of noise. By doing this, we utilize the gradual image generation process:

- (1) The later the final injection, the greater similarity of this fragment on the output to the input. As expected, because the fragment is changed by fewer iterations, the fewer changes are applied to this fragment.
- (2) The amount of noise added to the injected fragment is proportional to the number of steps that are to be applied to this fragment. The more steps a fragment will take part in, the more noise is added. This is a key change from the regular diffusion inference process, in which all the fragments are noised at the same time, and therefore should not be noised differently.

3.4.2 Future Hinting. It is tempting to assume, that it is enough to inject each fragment once, according to its designated strength. This might look reasonable as in most image-to-image translation procedures all the fragments are inserted on the first time-step. It also coincides with the observations made in Section 3.4.1, that lower-strength-fragments will be injected later. However, Throughout the new inference process, we re-inject some of the fragments repeatedly. On any time step k , we inject the fragments that correspond to k and the fragments that correspond to the *future* time-steps ($< k$), all noised by the quantity of k . Therefore, for the fragments with the lowest strengths, the process will inject their noised fragments many times, see: Figure 3. We called this behavior **future hinting**. This serves a few goals:

- (1) We give the diffusion model advance knowledge of some of the upcoming visual data, thereby allowing it to “plan” more complex objects. Meaning, we use that the model make decisions according the content of the entire picture.
- (2) Usually, diffusion models are trained on pictures that mostly contain no holes. Therefore, they are expected to be less robust to diffusion processes with blank pixels in their intermediate diffusion steps. Future hinting is a natural way to fill such holes with appropriate data.

We conducted a comparison experiment between our full method and a version without future hinting, meaning that for each time-step, only the fragments that match the exact time-step were injected (change Line 8 in Algorithm 1 to $mask = \frac{t+1}{k} \otimes \mu_s \otimes \frac{t}{k}$). The

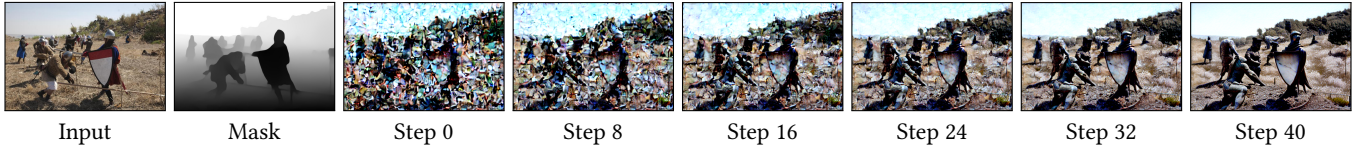


Fig. 2. In this figure we show the intermediate steps of *Differential Diffusion* inference process which uses “injection” in every time-step. As one can see, the injected content is indistinguishable from non-injected fragments as expected. Here the maximal strength is 30% and the lowest is 10%. The prompt is “statues of men”. We used the technique described in Section 3.5 to expand the prompt.

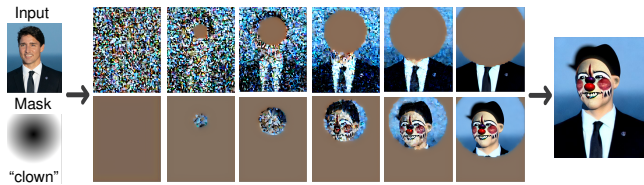


Fig. 3. On this figure, you can see the decomposition of the inference process of *Differential Diffusion*: Top: $z_{t+1} \odot \text{mask}$, which corresponds to the injected fragments at each time-step. bottom: $z_t \odot (1 - \text{mask})$ which corresponds to the fragments which are not injected at this time-step. Zero values are indicated in brown. As you can see, the low-strength fragments (the light ones) are injected across many time-steps, in contrast to the high-strength (dark) ones who are injected only in early and limited time-steps.

experiment demonstrates that future hinting improves result quality (Figure 6).

3.5 Technical Details

Model: We have used the checkpoint 512-base-ema.ckpt of Stable Diffusion 2.1.

Prompts: Our method uses standard Stable Diffusion prompts. For some experiments we used simple description of the editing. For others, we found it beneficial to take an existing image, reverse it to a prompt via clip interrogator which uses both BLIP [Li et al. 2022] and CLIP [Radford et al. 2021], and then add the desired edit to the prompt.

Masks: Our method does not assume anything about the source of the mask. We show results using various sources: Segment-anything [Kirillov et al. 2023], MiDaS [Ranftl et al. 2022] and manually drawn masks.

Other settings: Unless stated otherwise, we used 100 inference steps for each experiment.

4 RESULTS

Our method allows deliberate selection of which areas to edit and by how much. We found this controllability useful in many image editing tasks.

- **Heterogeneous Editing.** Editing in which different parts should change in different amounts. For example, given a picture of a pizza, adding varying amounts of toppings for each slice. (E.g., Figure 1 top-right, Figure 5).
- **Localized Style Transfer.** By entering an artistic prompt and a change map, a user can preserve most of the semantic content of important objects, while substantially changing

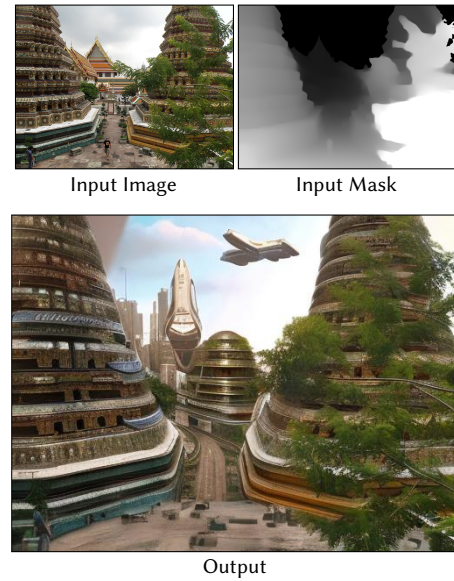


Fig. 4. An example of an output of *Differential Diffusion*. Notice the natural blend between the augmented part and the original one. Notice the minimal change to the trees, the subtle change to the pagodas, and the complete change of the background. In the map, black represents 50% change and white represents 0% change. The prompt is “a futuristic city”. We used the technique described in Section 3.5 to expand the prompts.

other regions, such as background objects. (E.g., Figure 1 top-left, Figure 2).

- **Convey Progression.** A user can show a process that is taking place in a picture, such as a burning forest or a decaying zombie. Different parts of the picture should burn/decay at different rates. (E.g., Figure 1 bottom-left, Figures 7 and 11).
- **Augmented Reality** A user can blend an artistic element into a photorealistic picture. By transitioning smoothly using the change map, the result looks more favorable. (E.g., Figure 1 bottom-right, Figure 4).

More results are shown in Figures 6, 10 and 11.

4.1 Comparisons

To the best of our knowledge, we are the first to use diffusion models for image editing with *strength variability*. Thus, we compare

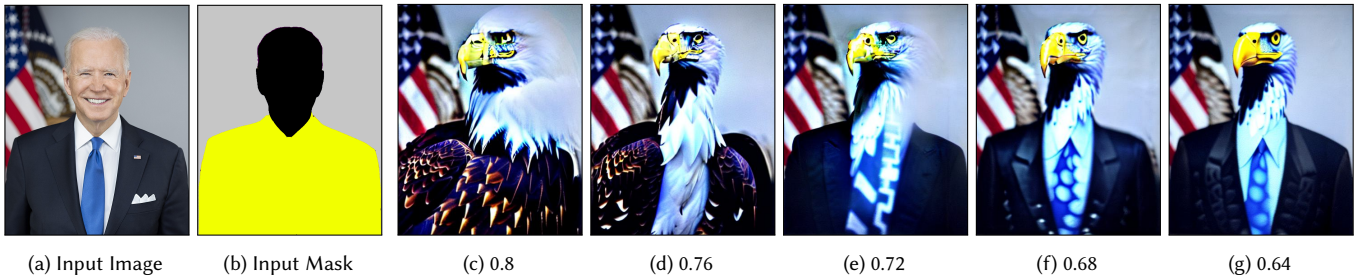


Fig. 5. In this experiment, we demonstrate the effect of strength on the editing process. a, b are the input to the model. On the mask, the yellow part varies according to the number listed below the illustration. The black represents full strength. The white represents no strength, everything in the middle will have its color accordingly linearly. c-g are the outputs of differential diffusion, whereas the yellow part is assigned the value listed below. As you can see, the stronger the strength, the greater the change. The prompt is “eagle”. We used the technique described in Section 3.5 to expand the prompt. All the pictures were created from the same seed for creating a gradual shift effect.



Fig. 6. Differential Diffusion with “Future Hinting” and without. As you can see, the output of the algorithm with “Future Hinting” is more complex, blend better with the scene, and less blurry. The 1st prompt is “a watercolor painting”. The 2nd prompt is “a fine art painting”. The 3rd prompt is “a city skyline with a lot of tall buildings at night time with lights on them and a large body of water in the background.”. The seed is fixed for each row. We used the technique described in Section 3.5 to expand the prompts.

against techniques that solve a problem close to ours — prompt-based inpainting. We compared with: (1) Stable Diffusion 2’s Text-Guided Inpainting [Stability AI Ltd 2023], and (2) Blended Latent Diffusion [Avrahami et al. 2022a] (Figure 10).

4.2 Evaluation

We evaluate our method’s adherence to the change map both qualitatively (Section 4.2.1) and quantitatively (Section 4.2.2).

4.2.1 Trend Reconstruction for single images. We would like to evaluate the adherence of our results to the change map. For example,

a map that changes gradually from one to zero should produce an image that is changed gradually, from fragments that hardly change at all, to fragments that are completely different from the input. There is an inherent relation between image content and the y-axis of the image. According to our experiments, all the techniques tend to favor editing at specific heights; this is expected. For example, a photograph of an upside-down tree, with its tree top at the bottom and its roots at the top, will be considered not photo-realistic. Thus, our measurement should take this into account, and cannot simply measure the pixel difference versus the target change map.

We suggest a **trend reconstruction** test — taking a *horizontal* gradient map and measuring whether the average *along the columns* changes linearly. Intuitively, we mostly care that the gradient map will be mimicked by the changes of the photo. The averaging along columns should also reduce measurement noise. Figure 7 shows that our results follow the gradient map.

4.2.2 Reliability score. Following the results in Figure 7, we wish to establish a numerical measure that quantifies this property, given the following considerations:

- (1) For all the methods we have examined, the results for a single image contained significant noise. This is expected, as the diffusion process is stochastic in nature.
- (2) All the methods we have examined are biased towards changing more in the fragments near the border of the picture.
- (3) Even if we change the entire picture (set the change map to zero for all pixels), some fragments will change to an output which is similar to the input, by pure coincidence.
- (4) The change map has a different scale and bias from pixel difference measurements (i.e., the trend should be similar, but the measurement units are not the same).

Therefore, we suggest the following metric. Given a dataset (a set of pictures) \mathcal{D} and a single change map μ of height h , an editing technique S , that accepts a picture to edit d , and μ a change map (for this experiment the text prompt is constant), and returns an edited image (3D tensor — height, width, channel). For each index i , the reconstructed trend $\tau_{\mathcal{D},\mu,S}$ is: $\tau_{\mathcal{D},\mu,S}[i] = \sum_{d \in \mathcal{D}} \frac{\|S(d,\mu)[:,i,:] - d[:,i,:]\|_2}{|\mathcal{D}|h}$. $\|\bullet\|_2$ is the L_2 norm, which outputs a scalar, “:” represents taking the entire indices in this dimension (like the Python slicing operator — “arr[:]). Due to the location-based bias explained above, we suggest subtracting the baseline trend: Given $\xi = 0_{h,w}$ (a matrix of 0s of dimension h, w) whereas h, w are the height width of μ (meaning ξ is the map of a complete change). We define the normalized trend as $\hat{\tau}_{\mathcal{D},\mu,S} = \tau_{\mathcal{D},\mu,S} - \tau_{\mathcal{D},\xi,S}$. Let G be the change map that satisfies: $\forall i(\forall j(G[i, j] = 1 - \frac{j}{h}))$, meaning G is a horizontal gradient change map. Given an editing method S , the reliability score of this method is: $R_{\mathcal{D},S} = \rho(\hat{\tau}_{\mathcal{D},G,S}, I)$, whereas I is a vector of the indices of the corresponding columns (In these settings it is $0 \dots w - 1$), and ρ is the Pearson correlation coefficient. The Pearson correlation coefficient is invariant to location and positive scale with two variables, which solves Item 4. In our experiments, we fixed \mathcal{D} : For testing, we have taken 5,000 randomly chosen pictures from the validation subset of ImageNet [Russakovsky et al. 2015]. All the models we tested take prompts for user-guidance. For these settings, we used the “” (empty string) as a prompt and negative prompts. We resize all the pictures to 512×512 , so they will be all at the same dimension (to fit the relative positions of the pictures). Blended-Diffusion and Stable-Diffusion 2’s Inpaint only accept binary mask values, so we used 0.5 as a threshold for change. We then calculate the suggested metric. The results are in Table 1 and Figure 8. Our results are better correlated with the change map, as evident in the graphs and by the higher Pearson correlation.

Table 1. Reliability Score (R) By Method

Method	R
Theoretical Limit	1
Stable Diffusion 2’s Inpaint	0.893
Blended Latent Diffusion	0.900
Ours	0.974

Table 2. Peak Memory consumption by method

Method	Peak VRAM
Stable Diffusion 2’s Img2Img	4555MB
Ours	4557MB

Table 3. We compared the memory which is used both by the regular, image-to-image inference process and ours (both use the same weights). As seen, the memory consumption is almost the same.

4.3 Memory Consumption

We measure the inference-time memory consumption of our technique versus the original Stable Diffusion’s image-to-image translation. Both share the same weights. on an NVIDIA GeForce RTX 3090, under the same settings. There is no significant difference in peak memory consumption, therefore, the overhead of using our algorithm is negligible (Table 2).

5 LIMITATIONS AND FUTURE WORK

We rely on latent-based diffusion models. Unfortunately, the encoding to the latent space is compressive, meaning that some of the original data, such as the exact color qualities and the exact visual fine-details, are lost in this process. Therefore, details of the input might not persist in the output, even in regions that we want to preserve. For future work, incorporating a fine-tuning process might alleviate the issue, as demonstrated in related works [Avrahami et al. 2022a]. Another drawback that emerges from the low dimension of the latent space is a cap on the resolution of the change map: the map is downsized to match the latent space’s dimensions. This can limit the ability to precisely edit small objects (less than 8 pixels for Stable-Diffusion’s settings).

Another limitation is if there is a great dissimilarity between the shape of the edited fragment and the shape of the hallucinated object (for example, an airplane and a rectangular Lego brick), the model might generate an object with artifacts on the outlines (see: Figure 9). We found this to be a rare phenomenon, and even for inputs which exhibit such behavior, using a different random seed solved the issue.

6 CONCLUSION

In this paper, we presented a new technique that enables fragment-wise control over the strength of the image-to-image translation process. Our method does not require neither optimization nor training, has a minimal overhead, and can be used with diverse images and prompts. We introduce new concepts: injection and

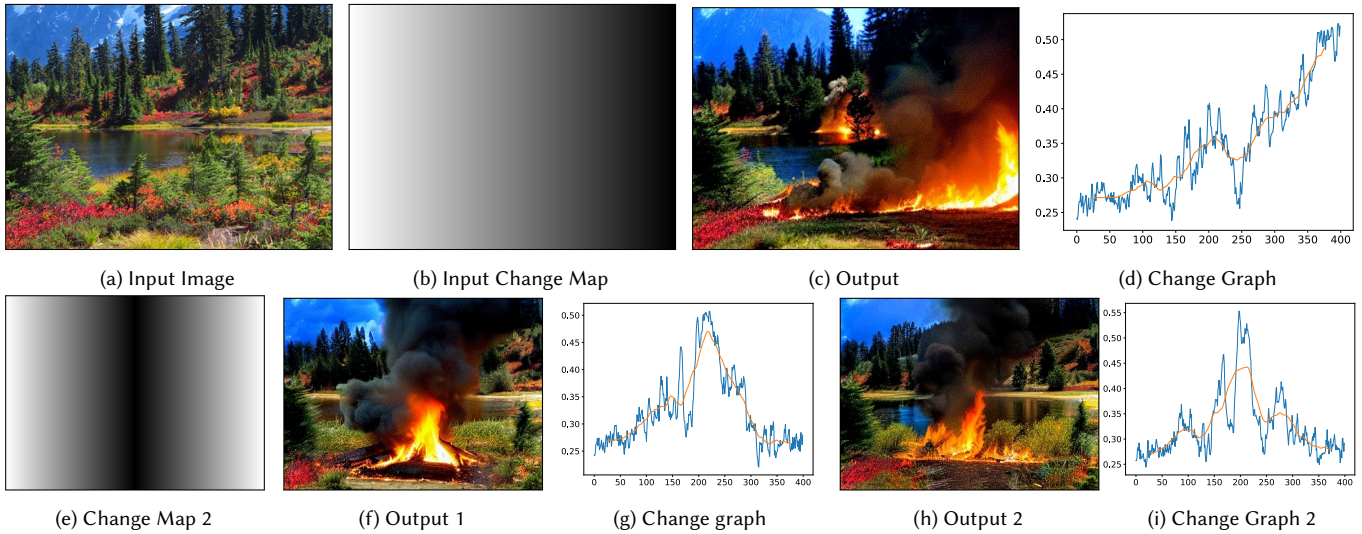


Fig. 7. Trend reconstruction for a single image. (Multiple of such experiments are used to calculate the reliability score in Table 1). Output 1 and Output 2 vary only by their seeds. We edit an image with the prompt “everything is burning, fire”. The change map is a horizontal gradient. Plots show the L_2 norm between input and output, averaged over each column (blue: raw result, orange: moving average). Our model adheres to the maps.

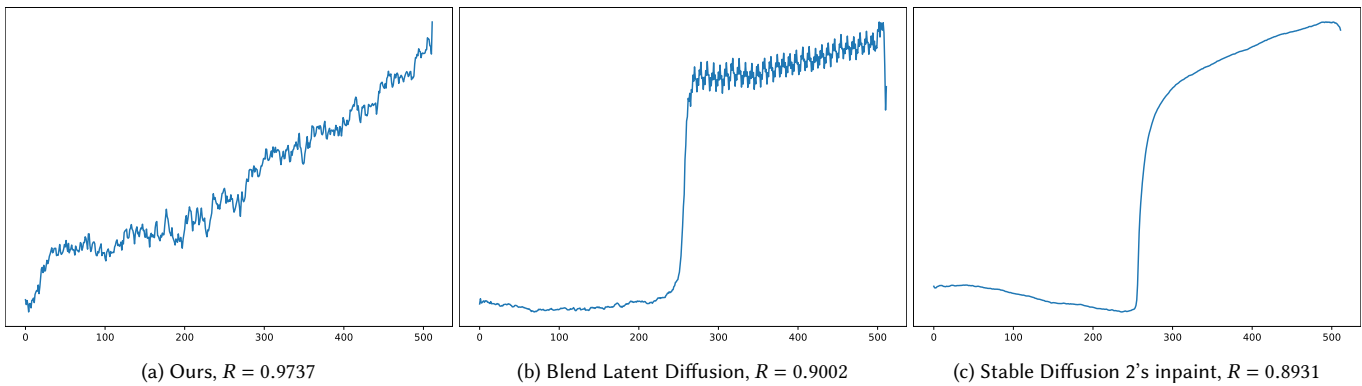


Fig. 8. A plot of the \hat{t} of different techniques. As seen, our technique adheres the most to the requested trend and therefore received the highest score. Note: By design, the reliability score is invariant to measurement unit (see Item 4). Therefore, the y-axis is not presented.

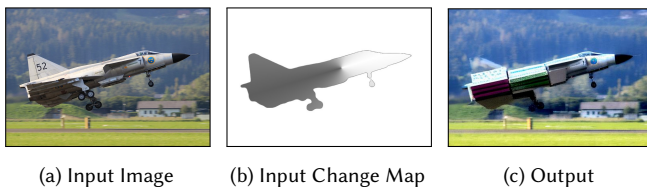


Fig. 9. Failure case. The rear wing in the left, was replaced, but an artifact is seen. As seen in Figure 11, using a different seed solves this issue.

future hinting, which can contribute to research in the field. Our work extends the scalar strength parameter into a more flexible 2D array, and we hope other researchers will extend this further.

ACKNOWLEDGMENTS

This work was supported in part by the Israel Science Foundation (grant No. 1574/21), and by the Tel Aviv University Center for AI and Data Science (TAD).

REFERENCES

- Martin Arjovsky, Soumith Chintala, and Léon Bottou. 2017. Wasserstein Generative Adversarial Networks. In *Proceedings of the 34th International Conference on Machine Learning (Proceedings of Machine Learning Research, Vol. 70)*, Doina Precup and Yee Whye Teh (Eds.). PMLR, 214–223. <https://proceedings.mlr.press/v70/arjovsky17a.html>
- Omri Avrahami, Ohad Fried, and Dani Lischinski. 2022a. Blended Latent Diffusion. arXiv:2206.02779 [cs.CV]
- Omri Avrahami, Dani Lischinski, and Ohad Fried. 2022b. Blended Diffusion for Text-driven Editing of Natural Images. In *2022 IEEE/CVF Conference on Computer Vision and Pattern Recognition (CVPR)*. IEEE. <https://doi.org/10.1109/cvpr52688.2022.01767>
- Omer Bar-Tal, Dolev Ofri-Amar, Rafail Fridman, Yoni Kasten, and Tali Dekel. 2022. Text2LIVE: Text-Driven Layered Image and Video Editing. arXiv:2204.02491 [cs.CV]

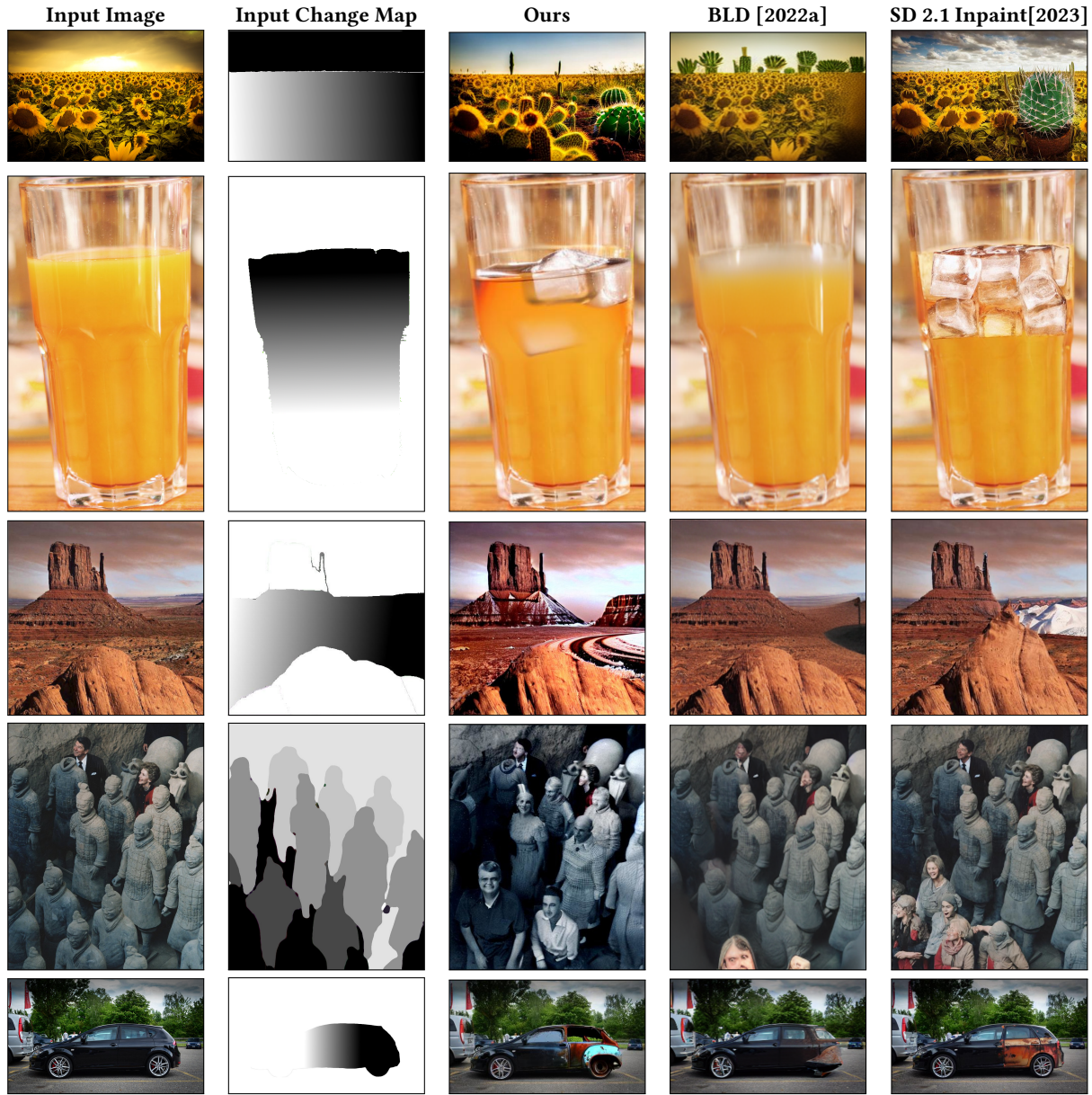


Fig. 10. Differential Diffusion versus Blend Latent Diffusion [Avrahami et al. 2022a] and Stable Diffusion 2.1’s Inpaint [Stability AI Ltd 2023]. 1st row: The prompt is “a cactus with fruit growing on it in a field”. As you can see, our approach minds the gradient, thus enabling a gradual shift from cacti (“cactuses”) to sunflowers. While other approaches do not offer any type of interpolation between the concepts; they just paste the cacti into the picture. In Blend Latent Diffusion, the cacti have not been pasted into the field. In Stable Diffusion 2’s Inpaint, a single cactus was put in the field, while presenting no gradual shifting. 2nd row: the prompt is “glasses with ice cubes”, all the other methods have failed to blend the ice with the juice, as such blend should be gradual. 3rd row: the prompt is “snowy surface”, one can see that our method adheres the most to the map. 4th row: the prompt is: “group of people are posing for a picture together”, one can see that only our method capture the transition from stones to human being, while on the other methods, only the first row is swapped. 5th row: the prompt is “rusted car”. One can see that the change in other methods is limited to a change in the color of the paint. We used the technique described in Section 3.5 to expand the prompts 1, 3, 4.

Tim Brooks, Aleksander Holynski, and Alexei A. Efros. 2023. InstructPix2Pix: Learning to Follow Image Editing Instructions. arXiv:2211.09800 [cs.CV]
 Prafulla Dhariwal and Alex Nichol. 2021. Diffusion Models Beat GANs on Image Synthesis. arXiv:2105.05233 [cs.LG]

Rinon Gal, Yuval Alaluf, Yuval Atzmon, Or Patashnik, Amit H. Bermano, Gal Chechik, and Daniel Cohen-Or. 2022. An Image is Worth One Word: Personalizing Text-to-Image Generation using Textual Inversion. arXiv:2208.01618 [cs.CV]

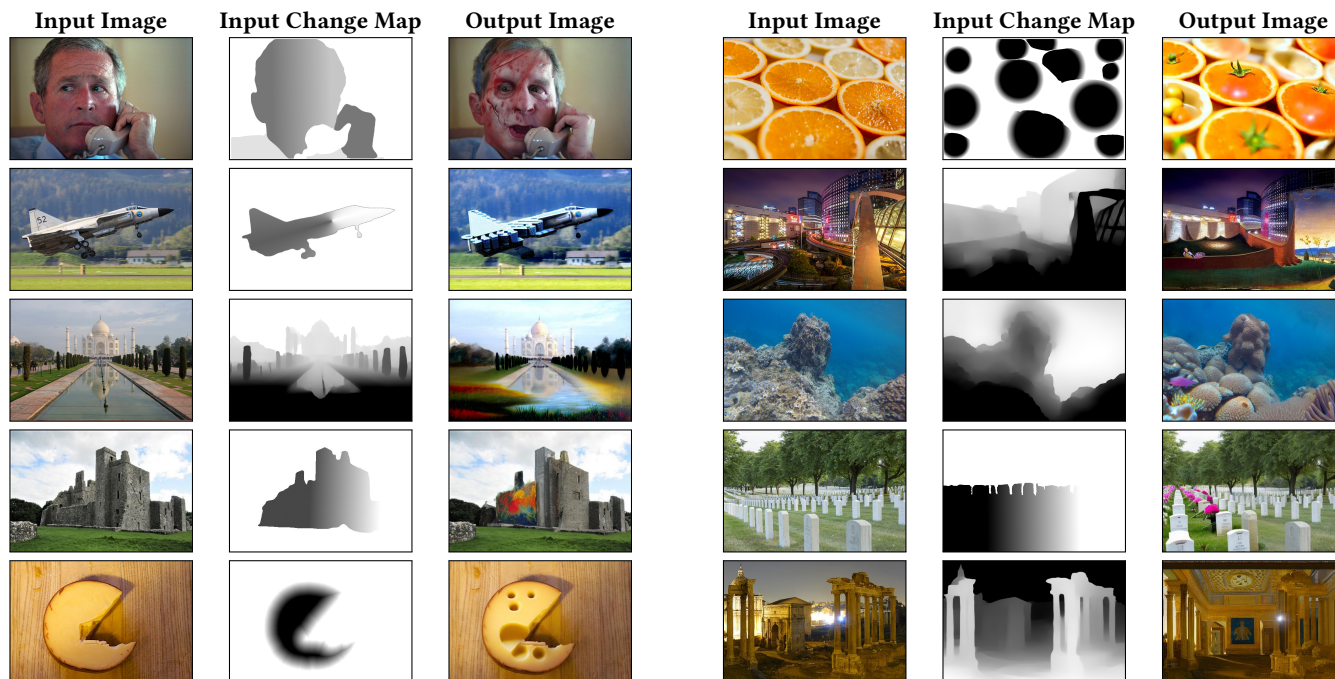


Fig. 11. Left to right, top to bottom, 1st row: the prompt is “zombie” with the negative prompt “” (empty string). The prompt is “a pile of tomatoes with green stems on them in a market place”. 2nd row: the prompt is “colorful lego blocks”. The prompt is “a detailed painting”. 3rd row the prompt is: “an oil on canvas painting, metaphysical painting”. The prompt is “Coral reef”. 4th row the prompt is “a painting with lots of paint splattered”. The prompt is “ouquets of flowers are placed in graves”, with the negative prompt”. 5th row the prompt is “Swiss cheese”. The prompt is “a mosaic”. We used the technique described in Section 3.5 to expand the prompt for the 2nd, 3rd, 4th, 5th, 6th, 8th examples.

Ian J. Goodfellow, Jean Pouget-Abadie, Mehdi Mirza, Bing Xu, David Warde-Farley, Sherjil Ozair, Aaron Courville, and Yoshua Bengio. 2014. Generative Adversarial Networks. arXiv:1406.2661 [stat.ML]

Karol Gregor, Ivo Danihelka, Alex Graves, Danilo Jimenez Rezende, and Daan Wierstra. 2015. DRAW: A Recurrent Neural Network For Image Generation. arXiv:1502.04623 [cs.CV]

Amir Hertz, Ron Mokady, Jay Tenenbaum, Kfir Aberman, Yael Pritch, and Daniel Cohen-Or. 2022. Prompt-to-prompt image editing with cross attention control. (2022).

Jonathan Ho, Ajay Jain, and Pieter Abbeel. 2020. Denoising Diffusion Probabilistic Models. arXiv:2006.11239 [cs.LG]

Bahjat Kawar, Shiran Zada, Oran Lang, Omer Tov, Huiwen Chang, Tali Dekel, Inbar Mosseri, and Michal Irani. 2023. Imagic: Text-Based Real Image Editing with Diffusion Models. arXiv:2210.09276 [cs.CV]

Gwanghyun Kim, Taesung Kwon, and Jong Chul Ye. 2022b. DiffusionCLIP: Text-Guided Diffusion Models for Robust Image Manipulation. arXiv:2110.02711 [cs.CV]

Soo Ye Kim, Kfir Aberman, Nori Kanazawa, Rahul Garg, Neal Wadhwa, Huiwen Chang, Nikhil Karnad, Munchurl Kim, and Orly Liba. 2022a. Zoom-to-Inpaint: Image Inpainting With High-Frequency Details. In *Proceedings of the IEEE/CVF Conference on Computer Vision and Pattern Recognition (CVPR) Workshops*. 477–487.

Alexander Kirillov, Eric Mintun, Nikhila Ravi, Hanzi Mao, Chloe Rolland, Laura Gustafson, Tete Xiao, Spencer Whitehead, Alexander C. Berg, Wan-Yen Lo, Piotr Dollár, and Ross Girshick. 2023. Segment Anything. arXiv:2304.02643 [cs.CV]

Junnan Li, Dongxu Li, Caiming Xiong, and Steven Hoi. 2022. BLIP: Bootstrapping Language-Image Pre-training for Unified Vision-Language Understanding and Generation. In *ICML*.

Xingchao Liu, Chengyue Gong, Lemeng Wu, Shujian Zhang, Hao Su, and Qiang Liu. 2021. FuseDream: Training-Free Text-to-Image Generation with Improved CLIP+GAN Space Optimization. arXiv:2112.01573 [cs.CV]

Xihui Liu, Dong Huk Park, Samaneh Azadi, Gong Zhang, Arman Chopikyan, Yuxiao Hu, Humphrey Shi, Anna Rohrbach, and Trevor Darrell. 2022. More Control for Free! Image Synthesis with Semantic Diffusion Guidance. arXiv:2112.05744 [cs.CV]

Andreas Lugmayr, Martin Danelljan, Andres Romero, Fisher Yu, Radu Timofte, and Luc Van Gool. 2022. RePaint: Inpainting Using Denoising Diffusion Probabilistic

Models. In *Proceedings of the IEEE/CVF Conference on Computer Vision and Pattern Recognition (CVPR)*. 11461–11471.

Elman Mansimov, Emilio Parisotto, Jimmy Lei Ba, and Ruslan Salakhutdinov. 2016. Generating Images from Captions with Attention. arXiv:1511.02793 [cs.LG]

Chenlin Meng, Yutong He, Yang Song, Jiaming Song, Jiajun Wu, Jun-Yan Zhu, and Stefano Ermon. 2022. SDEdit: Guided Image Synthesis and Editing with Stochastic Differential Equations. arXiv:2108.01073 [cs.CV]

Alex Nichol and Prallava Dhariwal. 2021. Improved Denoising Diffusion Probabilistic Models. arXiv:2102.09672 [cs.LG]

Or Patashnik, Zongze Wu, Eli Shechtman, Daniel Cohen-Or, and Dani Lischinski. 2021. StyleCLIP: Text-Driven Manipulation of StyleGAN Imagery. arXiv:2103.17249 [cs.CV]

Weize Quan, Ruisong Zhang, Yong Zhang, Zhifeng Li, Jue Wang, and Dong-Ming Yan. 2022. Image Inpainting With Local and Global Refinement. *IEEE Transactions on Image Processing* 31 (2022), 2405–2420. <https://doi.org/10.1109/TIP.2022.3152624>

Alec Radford, Jong Wook Kim, Chris Hallacy, Aditya Ramesh, Gabriel Goh, Sandhini Agarwal, Girish Sastry, Amanda Askell, Pamela Mishkin, Jack Clark, Gretchen Krueger, and Ilya Sutskever. 2021. Learning Transferable Visual Models From Natural Language Supervision. arXiv:2103.00020 [cs.CV]

René Ranftl, Katrin Lasinger, David Hafner, Konrad Schindler, and Vladlen Koltun. 2022. Towards Robust Monocular Depth Estimation: Mixing Datasets for Zero-Shot Cross-Dataset Transfer. *IEEE Transactions on Pattern Analysis and Machine Intelligence* 44, 3 (2022).

Scott Reed, Zeynep Akata, Xinchun Yan, Lajanugen Logeswaran, Bernt Schiele, and Honglak Lee. 2016. Generative Adversarial Text to Image Synthesis. arXiv:1605.05396 [cs.NE]

Robin Rombach, Andreas Blattmann, Dominik Lorenz, Patrick Esser, and Björn Ommer. 2022a. High-Resolution Image Synthesis with Latent Diffusion Models. arXiv:2112.10752 [cs.CV]

Robin Rombach, Andreas Blattmann, Dominik Lorenz, Patrick Esser, and Björn Ommer. 2022b. High-resolution image synthesis with latent diffusion models. In *Proceedings of the IEEE/CVF Conference on Computer Vision and Pattern Recognition*. 10684–10695.

Natanuel Ruiz, Yuanzhen Li, Varun Jampani, Yael Pritch, Michael Rubinstein, and Kfir Aberman. 2022. DreamBooth: Fine Tuning Text-to-image Diffusion Models for

- Subject-Driven Generation. (2022).
- Olga Russakovsky, Jia Deng, Hao Su, Jonathan Krause, Sanjeev Satheesh, Sean Ma, Zhiheng Huang, Andrej Karpathy, Aditya Khosla, Michael Bernstein, Alexander C. Berg, and Li Fei-Fei. 2015. ImageNet Large Scale Visual Recognition Challenge. *International Journal of Computer Vision (IJCV)* 115, 3 (2015), 211–252. <https://doi.org/10.1007/s11263-015-0816-y>
- Chitwan Saharia, William Chan, Huiwen Chang, Chris A. Lee, Jonathan Ho, Tim Salimans, David J. Fleet, and Mohammad Norouzi. 2022. Palette: Image-to-Image Diffusion Models. arXiv:2111.05826 [cs.CV]
- Axel Sauer, Tero Karras, Samuli Laine, Andreas Geiger, and Timo Aila. 2023. StyleGAN-T: Unlocking the Power of GANs for Fast Large-Scale Text-to-Image Synthesis. arXiv:2301.09515 [cs.LG]
- Jascha Sohl-Dickstein, Eric A. Weiss, Niru Maheswaranathan, and Surya Ganguli. 2015. Deep Unsupervised Learning using Nonequilibrium Thermodynamics. arXiv:1503.03585 [cs.LG]
- Stability AI Ltd. 2023. Stability.ai Blog: Stable Diffusion v2 Release. <https://stability.ai/blog/stable-diffusion-v2-release>. Accessed: April 25, 2023.
- Roman Suvorov, Elizaveta Logacheva, Anton Mashikhin, Anastasia Remizova, Arsenii Ashukha, Aleksei Silvestrov, Naejin Kong, Harshith Goka, Kiwoong Park, and Victor Lempitsky. 2022. Resolution-Robust Large Mask Inpainting With Fourier Convolutions. In *Proceedings of the IEEE/CVF Winter Conference on Applications of Computer Vision (WACV)*. 2149–2159.
- Tao Xu, Pengchuan Zhang, Qiuyuan Huang, Han Zhang, Zhe Gan, XiaoLei Huang, and Xiaodong He. 2017. AttnGAN: Fine-Grained Text to Image Generation with Attentional Generative Adversarial Networks. arXiv:1711.10485 [cs.CV]
- Tao Yu, Runseng Feng, Ruoyu Feng, Jinming Liu, Xin Jin, Wenjun Zeng, and Zhibo Chen. 2023. Inpaint Anything: Segment Anything Meets Image Inpainting. arXiv:2304.06790 [cs.CV]
- Chenshuang Zhang, Chaoning Zhang, Mengchun Zhang, and In So Kweon. 2023. Text-to-image Diffusion Models in Generative AI: A Survey. arXiv:2303.07909 [cs.CV]
- Han Zhang, Jing Yu Koh, Jason Baldridge, Honglak Lee, and Yinfei Yang. 2022. Cross-Modal Contrastive Learning for Text-to-Image Generation. arXiv:2101.04702 [cs.CV]
- Han Zhang, Tao Xu, Hongsheng Li, Shaoting Zhang, Xiaogang Wang, XiaoLei Huang, and Dimitris Metaxas. 2017. StackGAN: Text to Photo-realistic Image Synthesis with Stacked Generative Adversarial Networks. arXiv:1612.03242 [cs.CV]

A ADDITIONAL RESULTS

In our work we expanded some prompts as mentioned in the methodology section, by using BLIP [Li et al. 2022]. Appendix A.1 details the full prompts of the teaser in the main paper. The BLIP expansion mostly adds descriptions, but does not change the essence of the editing. Furthermore, we compared our result to results of other models using different random seeds, as seen in Figure 12. As the diffusion inference process is a probabilistic process, the seeds have significant impact on the output of the model. As the experiment shows, regardless of the seed, the other techniques cannot produce a realistic photo under these settings. Additionally, we found that for some edits, both a map and its inverse (without changing the other settings) can be useful, as demonstrated in Figure 13.

A.1 Teaser’s prompts

The following prompts were used in the teaser:

- (1) “a detailed matte painting, fantasy art, Christophe Vacher, matte fantasy painting”.
- (2) “a bunch of mushrooms on a pizza”.
- (3) “scaffolding”.
- (4) “a futuristic city with tall buildings and a lot of traffic in the foreground and a cloudy sky in the background, a detailed matte painting, afrofuturism, Beeple, cyberpunk city”.

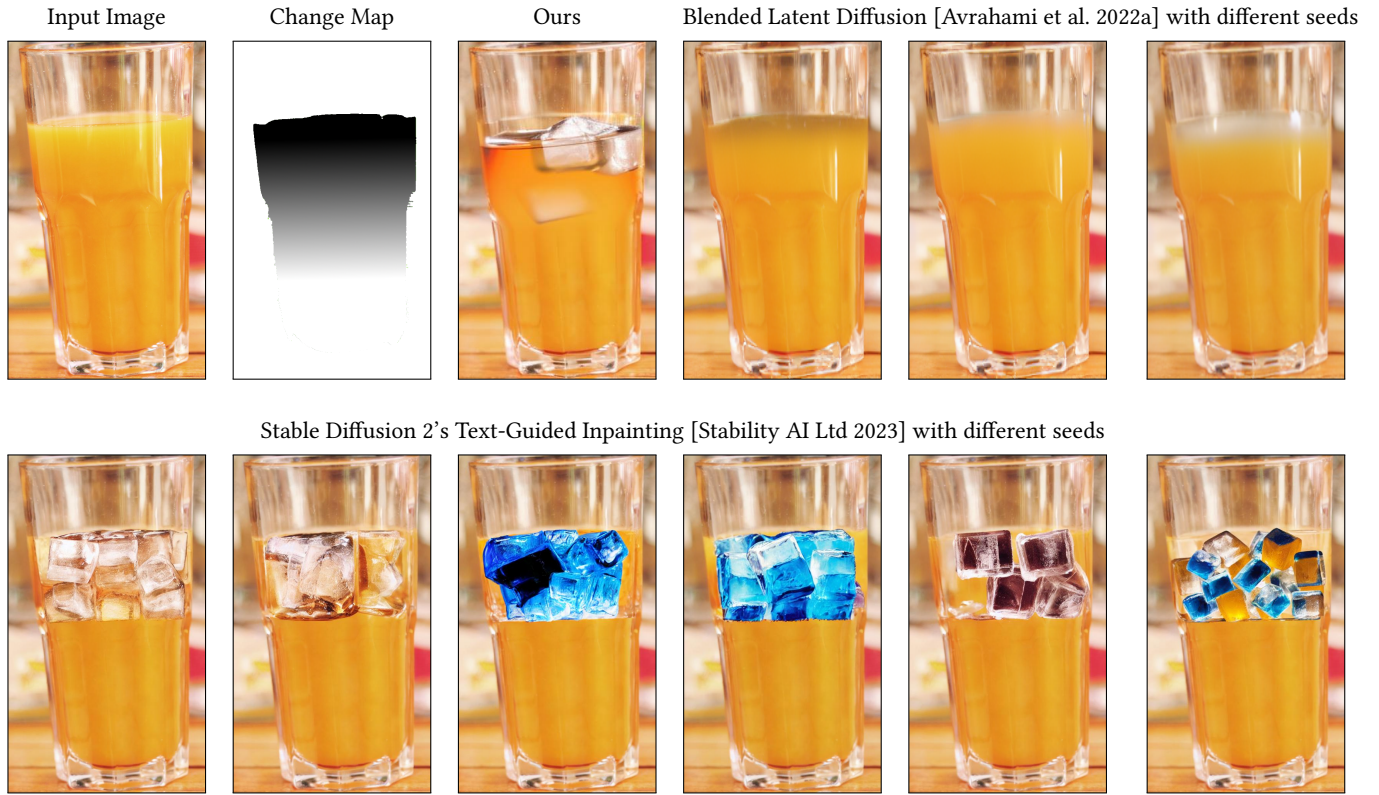


Fig. 12. Comparison of our result to other methods, using different random seed initializations. The prompt for all results is “glass with ice cubes”. Blended Latent Diffusion fails to generate ice-cubes, and Stable Diffusion cannot properly blend between the added cubes and the juice.

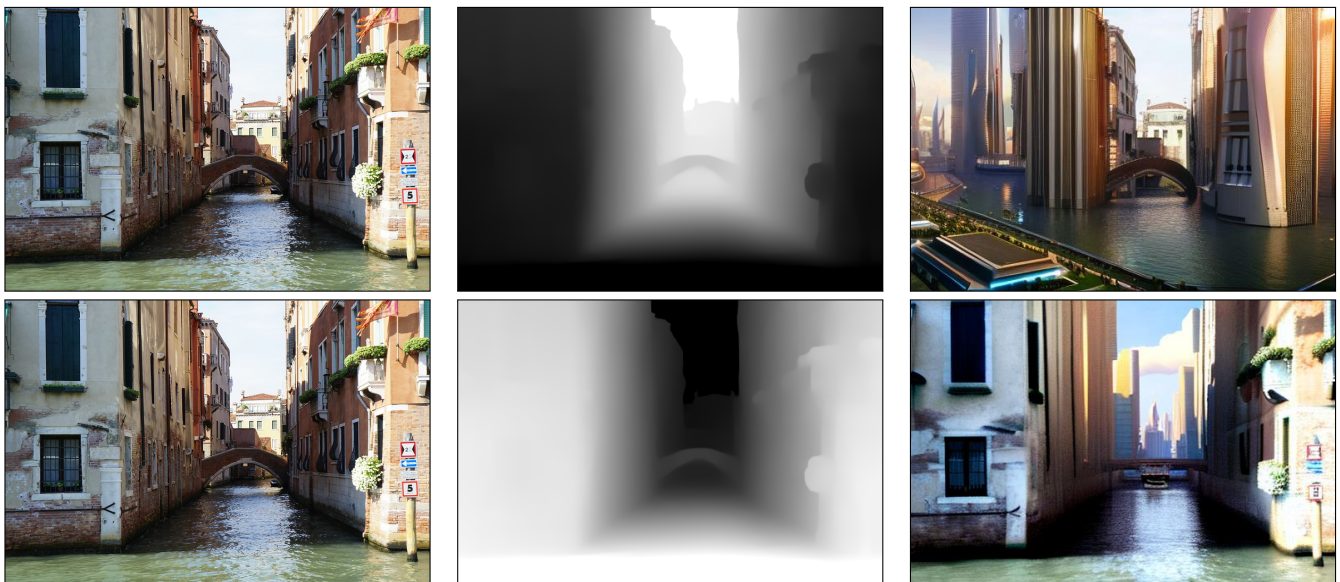


Fig. 13. For some edits, both the map (in this case, automatically extracted depth) and its inverse are useful.